C10_PE_Non-Contact_Temperature_Measurement.pdf

by Wipsar Sunu Brams Dwandaru

Submission date: 11-Dec-2021 11:03PM (UTC+0700)
Submission ID: 1727594559
File name: C10_PE_Non-Contact_Temperature_Measurement.pdf (1.79M)
Word count: 4891
Character count: 23899

PAPER

Phys. Educ. **55** (2020) 025017 (9pp) iopscience.org/ped

Non-contact temperature measurement based on Wien's displacement law using a single webcam in the infrared spectrum region

Saparullah, Agus Purwanto, Rhyko Irawan Wisnuwijaya, Emi Kurnia Sari and Wipsar Sunu Brams Dwandaru

Physics Education Department, Faculty of Mathematics and Natural Sciences, Universitas Negeri Yogyakarta, Jl. Colombo No. 1, Sleman, Yogyakarta, 55281, Indonesia

E-mail: ullah87@gmail.com, agus_purwanto@uny.ac.id, rhyko.irawan17@gmail.com, kurniasariemi@gmail.com and wipsarian@uny.ac.id

Abstract

The objective of this study is to design a temperature measurement system based on a non-contact method using a sensor camera from a webcam. The material being measured is nickel wire given an electrical current of 4.5 A–6.5 A with an interval of 0.5 A. The temperature measurement is based upon the measurement of the average pixel value distribution of infrared (IR) electromagnetic waves emitted by the measured material, i.e.: the nickel wire. The IR waves are passed through a diffraction grating and then captured by the sensor camera consisting of red, green, and blue layers. Calculation of the temperature is conducted by way of Planckian distribution as a model for the average pixel value distribution in the IR regions producing Wien's displacement law. Results show that the IR wavelength at maximum average pixel value shifts to a shorter wavelength as the nickel wire is heated in accordance with Wien's displacement law. Moreover, the Wien's constant is recovered for the temperature calculation of the red and green layers, which shows the best model for the non-contact measurement system. However, the temperature measurement still contains a systematic error that shifts the calculated temperature in contrast to the true temperature. This systematic error may be reduced by adjusting the measurement system set-up.

1. Introduction

In the past two decades, the industrial world has developed a new method of temperature measurement by processing thermal images from infrared (IR) radiation [1]. This method is often also referred to as thermography [2]. The application of this method is conducted widely in scientific research and industry as a novel non-destructive testing [3], monitoring [2–4], and gas type testing [5] method. Non-contact thermal imaging has the ability of remote measurement without direct contact with the object being measured, e.g. measuring the depth of a thick oil spill [6] and breathing rate [7]. Thermal imaging may replace conventional thermometer in the temperature measurement of a material.

Digital cameras [8] are always equipped with sensors built from semiconductor materials that are sensitive to certain wavelengths of photons. Sensors built with silicon material will be sensitive to photons with wavelengths below 1.1 μm, which includes visible light at wavelengths of 0.4 μm to 0.8 μm. Therefore, every digital camera is equipped with filters that pass only visible light wavelengths. Basically, every digital camera can be used as a near infrared (NIR) sensor by removing the filter that passes only visible light and installing filters that pass only infrared.

Planck's black-body law [9, 10] states that each distribution curve (representing a certain temperature, T) has a maximum value at a certain wavelength ($\lambda_{\max}$). Subsequently, Wien's displacement law states that the relationship between $\lambda_{\max}$ and T results in a constant called the Wien's constant. The aforementioned relationship between $\lambda_{\max}$ and T can be derived from the equation of the intensity distribution of the Planckian distribution. Planck states the intensity equation for the black body radiation as:

$$I_{b,\lambda} = \frac{C_1 \lambda^{-5}}{\left[e^{\frac{C_2}{\lambda T}} - 1\right]} \tag{1}$$

where C_1 and C_2 are constant parameters. If equation (1) is differentiated with respect to the wavelength, λ, set to be equal to zero, i.e.: $\frac{dI_{b,\lambda}}{d\lambda} = 0$, then the value of $\lambda_{\max} T$ is always constant or $\lambda_{\text{peak}} T = b$ with b equal to 2.898×10^6 nmK. This value of b is known as Wien's constant.

Thermal image processing makes use of NIR radiation so that anyone can make their own thermal camera using an ordinary digital camera by removing the IR filter and installing a visible light filter. Image processing captured by the digital camera that functions as an IR camera can be done based on the Planckian distribution. The purpose of the present study is to design a thermal camera for temperature measurement in a non-contact manner based on the Planckian distribution and subsequently the Wien's displacement law in the IR regions. Hence, this measurement system can be an excellent school project for senior high school students or a final year project for undergraduate students.

2. Method

The study is experimental research carried out to determine the wavelengths at peak intensities ($\lambda_{\max}$) induced by changes in the electrical current (I) subjected upon a nickel wire such that the nickel wire is heated. The data obtained are then plotted to determine the temperature (T) of the heated nickel wire based on Planckian-like distribution, especially in the near infra-red (NIR) region.

The heated material being observed is the nickel wire, which is made in the form of a solenoid with 17 coils each of which is 9 mm in diameter. The wire is then electrified on a direct current (DC) such that heat is produced. The heat arises from the wire while emitting electromagnetic waves. The current is varied in a range between 4.5 A and 6.5 A with an interval of 0.5 A.

The radiation of the electromagnetic waves emitted by the wire is observed using a web camera (webcam) for each variation of the current. The webcam is equipped with a thin filter sensor on the surface of the pixel that serves to draw up the colour of the object so that the image from the webcam consists of three layers, i.e.: red, green, and blue (RGB). The sensor is a camera sensor with an array size of 1280x720. The size of this array shows that the camera sensor has a length of 1280 pixels and a width of 720 pixels. Moreover, before being received by the webcam, the electromagnetic waves are passed through a diffraction grating.

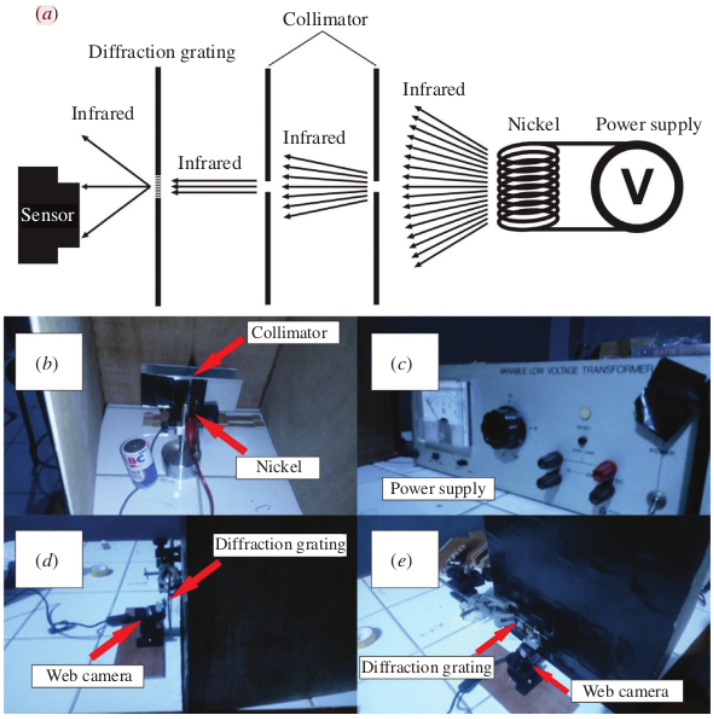

Figure 1. Illustration of the device arrangement (a), side view of the device (b), the power supply (c), the webcam and diffraction grating from side view (d) and top view (e).

A graphical illustration of the experiment setting is provided in figure 1(a). The experiment is carried out in the following steps: (i) placing the nickel coils in an (light-tight) enclosed box to avoid noise on the webcam sensor (figure 1(b)), (ii) connecting the nickel wire to a power supply as the electrical source (figure 1(b)), (iii) placing two collimators in front of the nickel coils (figure 1(b)), (iv) placing a diffraction grating outside the box in front of the collimator (figure 1(d)), (v) placing the webcam outside of the box parallel exactly in front of the grating (figure 1(c)), (v) turning ON the power supply connected to the nickel wire such that the nickel wire is heated, (vi) the spectral emitted by the heated nickel wire are captured and observed by the webcam, and (vii) analyzing the IR spectral from the webcam to determine the temperature of the heated nickel wire. The tools used in this study must be sterile from vibrations so that the position of each tool does not change relative to each other. The diffraction grating used is a grid with 600 lines per mm. Hence, the width of the gap in the grating is 1.67 micrometers. Finally, the distance of the webcam from the grating is 6.7 mm.

The camera sensor is so placed that the centre and first bright diffraction patterns can be captured by the sensor. The pattern is then analyzed to determine the maximum wavelength at each value of the current flowing in the nickel wire. Determining the maximum wavelength value is done by taking the pixel value data on the first bright pattern and then plotting it according to the wavelength. This data can be used to determine the temperature of the heated nickel wire.

The analysis to obtain the distribution of the IR spectral from the webcam may be explained as follows. The index of the centre bright pixel is determined from the midpoint of the pixel index range with the largest pixel value. The first order

bright pattern, t_1, is determined from a range of indices observed from the pixel pattern forming a band. The distance of the centre and the first order bright patterns, P, is determined by the difference between the centre and first-order bright pixel indices (in pixel units), stated mathematically as $P = |t_p - t_1|$. In this study, the pixel index with a length of 1280 is used as a 'ruler bar' to measure P in order to calculate the wavelength produced by the wire. The central bright pattern in this study is located in the pixel with an index of 1139, whereas the first-order bright pattern is located in the pixels with a range of indices from 80 to 500. However, the unit of the wavelength obtained is still in pixels and needs to be converted into nanometre (nm). To change the pixel unit into nm, P must be multiplied by the pixel width, δ_p, in nm. The pixel width in nm is determined by the width of the sensor, δ_s, divided by the number of pixels, k, or it can be stated as $\delta_p = \delta_s/k$. Hence, the value of P in nm, that is P_n can be determined via $P_n = P\delta_p$. Converting the length of 1280 pixels into meters is done by measuring the length of the sensor using a calliper, resulting in a length of one-pixel equivalent to 4687.5 nm.

The wavelength range is determined using the equation

$$n\lambda = d\sin\theta, \tag{2}$$

with

$$\sin\theta = \frac{P_n}{(P_n^2 + L^2)^{\frac{1}{2}}}, \tag{3}$$

with $n = 1$ (first-order bright pattern), such that

$$\lambda = d\,\frac{P_n}{(P_n^2 + L^2)^{\frac{1}{2}}}. \tag{4}$$

Using this equation, the wavelength of the pixel range of 80 to 500 is 680.2 nm to 992.2 nm. Pixel value data obtained from the image captured by the camera sensor are summed and then divided by the number of the data available to obtain the average pixel values. The average pixel values are then plotted on a graph to determine the distribution pattern of the infrared intensity as a function of the wavelength.

In order to determine the temperature of the nickel wire, we propose that the aforementioned IR pixel distribution is in accordance with a Planckian-like black body distribution. The reason is that the infrared radiation emitted by nickel wire is a thermally induced radiation, such that its pixel distribution should be similar to that of the black-body distribution, although the nickel wire itself may not be an ideal black-body. Hence, the pixel distribution can be stated in λ following equation (1) where C_1 and C_2 may be determined by fitting the pixel distribution data with equation (1). However, in this case, these parameters are not explicitly calculated. Furthermore, the Wien's displacement law is also obtained as given above. As in the black-body, the Wien' displacement law should not depend upon the shape or material of the radiator [11], but certainly depends upon the measuring device used. The Wien's displacement law is the main relation for the non-contact temperature measurement system, i.e.: measuring the λ_{max} of the material produces its temperature, T, with b being the Wien's constant and can be written as

$$\lambda_{max}T = b. \tag{5}$$

Hence, in order to apply the equation, the constant b must be determined from the measurement process. In this case, b is determined by comparing the λ_{max} obtained from the webcam measurement with the true temperature obtained from a contact temperature measurement via a thermocouple. Once b is obtained, then the Wien's displacement law can be used to determine the temperature of any (heated) material using this specific measurement system.

The temperature measurement using a thermocouple may be given as follows. First, the thermocouple is calibrated using a furnace. This is conducted by placing the thermocouple inside the furnace. Then, the temperature of the furnace is set. For each value of the furnace temperature, the voltage of the thermocouple is measured. Hence, a graph between the temperature and voltage (T versus V) can be produced. In order to measure the temperature of the nickel wire, the thermocouple is placed inside the nickel coil. As the nickel wire is heated, the thermocouple produces a voltage, which then can be compared to the T versus V graph obtained. Finally, using the λ_{max} data from the non-contact (webcam) measurement and T from the contact (thermocouple) measurement, the constant K may be measured.

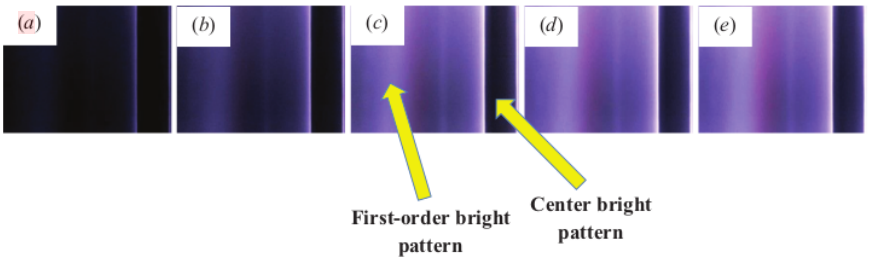

Figure 2. Images of the IR spectral captured by the webcam with 4.5 A (a), 5.0 A (b), 5.5 A (c), 6.0 A (d), and 6.5 A (e) of the electrical current given to the nickel wire.

3. Results and discussion

The diffraction patterns of the electromagnetic waves emitted by the hot wire are captured by the webcam, especially in the IR spectral range. The images which are captured by the webcam sensor are stored as RGB images in a jpg. format. These images may be observed in figure 2 with various electrical current values.

Figure 2 shows the diffraction patterns of the electromagnetic waves emitted by the heated nickel wire. It can be observed from the images that the centre bright pattern is located on the right side of each of the image given by the dark area as indicated by the arrow. This pattern becomes dark because it is intentionally covered to manually control the automatic gain control (AGC) so that it appears to resemble a solar eclipse in that it may not out-bright the first-order bright pattern. The first-order bright pattern is located on the left side of each image as indicated by the yellow arrow. Furthermore, it may be observed that, as electrical current is increased, the image becomes brighter.

Figure 3 present the results of the data plotting that have been processed. These are graphs of the average pixel values as functions of the pixel positions (left) and wavelengths (right) for red (a), green (b), and blue (c) layers, respectively. The average pixel values versus the wavelengths (right) graphs are obtained by converting the pixel positions to wavelengths as explained above. The range of the wavelength obtained is in the range of the visible to the NIR spectral, i.e.: from 600 nm to 1000 nm. The RGB layers show similar behaviour for the distribution of the average pixel values, that is starting from wavelengths of around 1000 nm the average pixel values increase and until a certain wavelength the average pixel values reach a peak (maximum value), and then decreases as the wavelengths become shorter. It may also be observed that the peak of each distribution tends to shift to the left (lower wavelengths) as the electrical current is increased (figure 3-right). This result is as expected: as the electrical current is increased, the higher the temperature and the brighter the nickel wire becomes as observed in figure 2, which means that the wavelengths at the maximum intensity of the average pixel values should shift to shorter wavelengths [12, 13]. It may also be observed that, as the electrical current is increased, the temperature increases, and the distribution tends to shift upward (higher average pixel values). The behaviours illustrated in the graphs are similar to those of the intensity distribution for the black-body [14]. However, in reality, no object behaves like an ideal black-body, including the nickel coil. It is not a perfect black-body although the radiation produced here is thermally induced [15]. Therefore, a Planckian distribution is proposed as given by equation (1) for the distributions in figure 3 in terms of C_1 and C_2. Consequently, the Wien's displacement law may be obtained but with constant b depending upon the device used to measure the pixel values. Hence, the latter is used as the basis of the non-contact temperature measurement using a webcam in the IR regions.

The wavelength at the maximum average pixel value for each electrical current and RGB layers may be observed in table 1. For the electrical current variation from 4.5 A to 6.5 A, the wavelengths at the maximum average pixel values are 840.0 nm to 811.7 nm, 853.4 nm to 815.6 nm, and 842.2 nm to 817.1 nm for the RGB layers, respectively. These wavelength values are clearly in the NIR regions. Furthermore, it is confirmed that, as

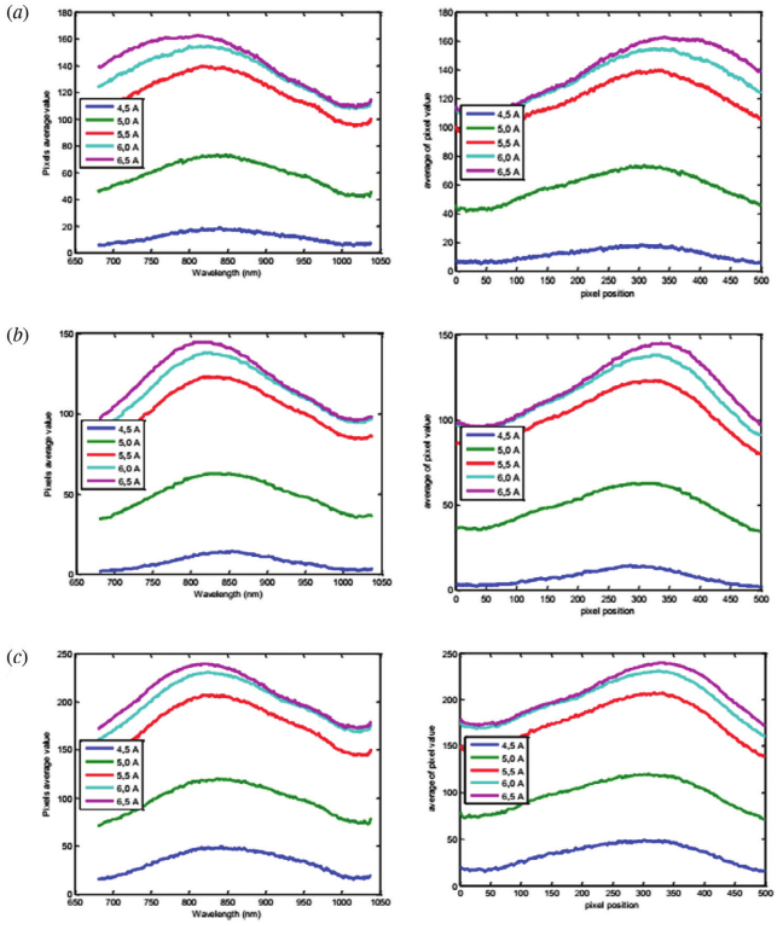

Figure 3. The distribution curves of the average pixel value as a function of the wavelength for the red (a), green (b), and blue (c) layers.

the current is increased, the values of these wavelengths decrease (to lower values).

On the other hand, the current flowing through the wire is converted into temperature measured using a thermocouple. This is done to compare the results of the above measurement with the contact temperature measurement in order to establish the non-contact measurement system. The calibration of the thermocouple, which is placed inside the furnace, produces a linear relation between the furnace temperature and the thermocouple voltage as given in figure 4. The voltage measurement of the thermocouple is done by positioning the thermocouple inside the nickel wire, and once the voltage is obtained it is converted into temperature using figure 4. The results of the voltage of the heated nickel wire and the temperature produced for each electrical current variation may be observed in table 1, especially columns 4, 8, and 9. It can be seen that, as

Table 1. The comparison between the wavelength at the maximum average pixel value and the temperature (thermocouple) as a function of the current.

No.	Current (A)	1/A	Thermocouple voltage (mV)	Wavelength at maximum average pixel value (nm)			Temperature from thermocouple	
				Red layer	Green layer	Blue layer	(°C)	(K)
1	4.5	0.22	12.7	840.0	853.4	842.2	379.5	652.5
2	5	0.2	14.1	837.0	830.9	836.2	407.7	680.7
3	5.5	0.18	15.9	815.6	820.2	828.6	444.0	717.0
4	6	0.17	17.9	815.6	820.2	824.0	484.3	757.3
5	6.5	0.15	21.1	811.7	815.6	817.1	548.7	821.7

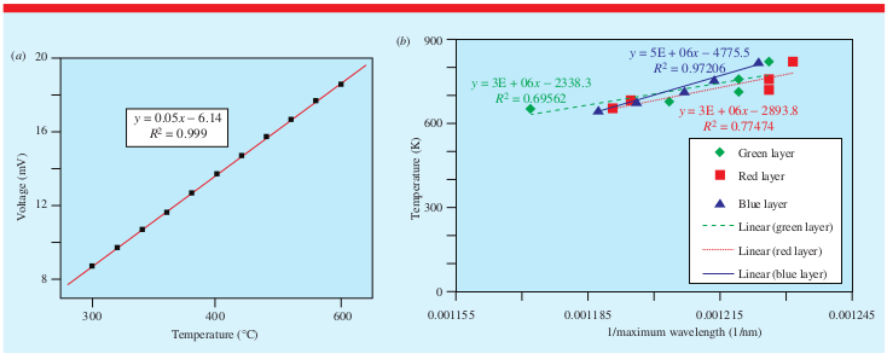

Figure 4. The calibration results of the furnace temperature with the voltage of the thermocouple (a) and the graph of the temperature T versus $1/\lambda_{max}$ obtained from from the data of table 1 (b).

the current is increased, the thermocouple voltage increases as well; hence, the temperature of the nickel wire increases.

To establish a relationship between the wavelength at maximum average pixel values (table 1: columns 5, 6, and 7) and the thermocouple temperatures (columns 8 and 9) as the basis for the non-contact temperature measurement system, the Wien's displacement law is utilized. The constant b is perceived that satisfies the relationship between λ_{max} and T based on results obtained in table 1. This constant can be determined by plotting T (in Kelvin) as a function of $1/\lambda_{max}$ (in 1/nm) from table 1, which should produce a straight line given in figure 4(b). Subsequently, the gradient of the line is b. Figure 4(b) shows the results of plotting T versus $1/\lambda_{max}$ for the RGB layers. Based on figure 4(b), the constant b for the red and green layers is 3×10^6 nmK, whereas, for the blue layer, it is 5×10^6 nmK. Comparing the aforementioned b results with the Wien's constant of 2.897×10^6 nmK [16], it may be observed that the b for the red and green layers produces a good agreement with the Wien's constant, whereas, for the blue layer, it is almost twice of the Wien's constant. The red and green layers produce consistent results with Wien's displacement law because these colour layers are closer to the IR spectrum compared to the blue layer, hence more sensitive in capturing the IR electromagnetic waves. On the other hand, the blue layer produces the best fit as the value of the R^2, viz. 0.97; it is closest to 1.00, compared to the red and blue lines.

The linear fit in figure 4 for all layers produces an additional term C_3, such that the formula becomes

$$T = K\left(\frac{1}{\lambda_{max}}\right) + C_3, \tag{6}$$

which does not exactly correspond to equation (5). This discrepancy may be remedied by moving C_3 to the LHS of equation (6) and denoting $T - C_3$ as the colour temperature [17–19] or T_c, equation (5) becomes

$$T_c = K\left(\frac{1}{\lambda_{max}}\right), \quad (7)$$

which is now in accordance with the Wien's displacement law of equation (5). Now, equation (7) indicates that T_c in equation (7), which satisfies the Wien's displacement law is not the true temperature of the material being measured. Moreover, the true temperature (T) is obtained by calculating T_c from the Wien's displacement law of equation (7) and then subtracting T_c by the value of C_3. In error analysis [20], the fact that T_c is not the true temperature shows that C_3 is a systematic error in this non-contact measuring system. This can be explained as the tools of the measuring system are built partially which produce imprecision in the measurement. Hence, the value of C_3 may be reduced by the following ways, e.g.: applying a better position setting of the object, collimator and the diffraction grating of the non-contact measuring system and making sure that the components of the measuring system do not vibrate or displaced when the measurement is conducted. It is also important to always positioned the sensor (webcam) such that it only captures one side of the diffraction pattern as the pixel length is limited (see the left-most part of figure 1(a)).

4. Conclusion

The design of the non-contact temperature measurement system is built using a webcam camera as a heat sensor that captures the diffraction pattern of electromagnetic waves (from the observed material) passed through the diffraction grating. Before passing through the grating, the electromagnetic wave is first passed through the collimator to produce a parallel wave beam. The webcam captures the average pixel value distribution, which results in the wavelength at the maximum average pixel value to shift to a shorter wavelength as the current given to the nickel wire is increased. Based on the Planckian distribution of the average pixel values, the Wien's constant is recovered for the red and green layers, which is the best model to be used as the basis for this temperature measurement system. The systematic error that is contained in T_c may be reduced by better arrangement of the measurement system set-up. Further observation in order to reduce the aforementioned systematic error includes (i) setting the camera sensor without the AGC feature so that the intensity received by the sensor does not experience electronic gain; (ii) providing more precision to the device concerning the sensor, diffraction grating, and collimator; and (iii) building a prototype in a box that cannot pass IR radiation in order to prevent noise from outside the device.

Acknowledgments

The authors would like to thank the Faculty of Mathematics and Natural Sciences, Universitas Negeri Yogyakarta for funding this study.

ORCID iDs

Wipsar Sunu Brams Dwandaru https://orcid.org/0000-0002-9692-4640

Received 5 November 2019, in final form 23 December 2019
Accepted for publication 9 January 2020
https://doi.org/10.1088/1361-6552/ab69b7

References

[1] Rogalski A and Chrzanowski K 2002 Infrared devices and techniques *Opto-Electron. Rev.* **10** 111–36
[2] Bagavahiappan S, Lahiri B B, Saravanan T, Philip J and Jayakumar T 2013 Infrared thermography for condition monitoring—a review *Infrared Phys. Technol.* **60** 35–55
[3] Usamentiaga R, Venegas P, Guerediaga J, Vega L, Molleda J and Bulnes F G 2014 Infrared thermography for temperature measurement and non-destructive testing *Sensors* **14** 12305–48
[4] Lietta E, Colucci D, Distefano G and Fissore D 2019 On the use of infrared thermography for monitoring a vial freeze-drying process *Sciences* **108** 391–8
[5] Nau P, Yin Z, Lammel O and Meier W 2018 Wall temperature measurements in gas turbine combustors with thermogaphic phosphors *J. Eng. Gas Turbines Power* **141** 1–9
[6] Allik T H, Dixon R E and Walters M 2018 Remote measurement of thick oil spill depth using thermal imagery *Proc. SPIE* **10631** 106310F
[7] Hu M, Zhai G, Li D, Li H, Liu M, Tang W and Chen Y 2018 Influence of image resolution on the performance of remote breathing rate measurement using thermal maging technique *Infrared Phys. Technol.* **93** 63–9
[8] Maitre H 2015 *From Photon to Pixel* (New York: Wiley)

[9] Tsallis C, SáBarreto F C and Loh E D 1995 Generalization of the Planck radiation law and application to the cosmic microwave background radiation *Phys. Rev.* E **52** 1447–51
[10] Choudhury S L and Paul R K 2018 A new approach to the generalization of Planck's law of black-body radiation *Ann. Phys.* **395** 317–25
[11] Passon O and Grebe-Ellis J 2017 Planck's radiation law, the light quantum, and the prehistory of indistinguishability in the teaching of quantum mechanics *Eur. J. Phys.* **38** 035404
[12] Khan N, Abas N and Kalair A 2016 Multiline distributed feed back dye laser endorses Wien's displacement law *Appl. Phys.* B **122** 3–4
[13] Fisenko A I and Ivashov S N 1999 Determination of the true temperature of emitted radiation bodien from generalized Wien's displacement law *J. Phys. D: Appl. Phys.* **32** 2882–5
[14] Zhang Z M and Wang X J 2010 Unified Wien's displacement law in terms of logarithmic frequency or wavlength scale *J. Thermophys. Heat Transfer* **24** 222–4
[15] Liu X, Tyler T, Starr T, Starr A F, Jokerst N M and Padilla W J 2011 Taming the blackbody with infrared metamaterial as selective thermal emitters *Phys. Rev. Lett.* **107** 045901
[16] Particle Data Group 2008 Constants, units, atomic and nuclear properties *Phys. Lett.* B **667** 103–15
[17] He G and Zheng L 2010 Color temperature tunable white-light light-emitting diode clusters with high color rendering index *Opt. Soc. Am. Appl. Opt.* **49** 470–6
[18] Thevenet J, Siroux M and Desmet B 2010 Measurements of brake disc surface temperature and emmisivity by two-color pyrometry *Appl. Therm. Eng.* **30** 753–9
[19] Gardner J L 2000 Correlated colour temperature-uncertainty and estimation *Metrologia* **37** 381–4
[20] Gabriel C and Peyman A 2006 Dielectric measurement: error analysis and assesment of uncertainty *Phys. Med. Biol.* **51** 6033–46

Saparullah is a student of the Department of Physics Education, Graduate School of Universitas Negeri Yogyakarta, Jl. Colombo No.1,Sleman, Yogyakarta 55281, Indonesia.

Agus Purwanto is a Lecturer (MSc) of the Department of Physics Education, Faculty of Mathematics and Natural Sciences, Universitas Negeri Yogyakarta, Jl. Colombo No.1, Sleman, Yogyakarta, Indonesia.

Rhyko Irawan Wisnuwijaya is a student of the Department of Physics Education of Graduate School Universitas Negeri Yogyakarta, Jl. Colombo No.1, Sleman, Indonesia.

Emi Kurnia Sari is a student of the Department of Physics Education, Graduate School of Universitas Negeri Yogyakarta, Jl. Colombo No.1, Sleman, Indonesia.

Wipsar Sunu Brams Dwandaru is a Lecturer (PhD) of the Department of Physics Education, Faculty of Mathematics and Natural Sciences, Universitas Negeri Yogyakarta, Jl. Colombo No.1, Sleman, Indonesia.

C10_PE_Non-Contact_Temperature_Measurement.pdf

ORIGINALITY REPORT

12%	9%	10%	3%
SIMILARITY INDEX	INTERNET SOURCES	PUBLICATIONS	STUDENT PAPERS

PRIMARY SOURCES

1	eric.ed.gov Internet Source	3%
2	Himawan Putranta, Yusman Wiyatmo, X X Supahar, Wipsar Sunu Brams Dwandaru. "A simple liquid density measuring instrument based on Hooke's law and hydrostatic pressure", Physics Education, 2020 Publication	2%
3	Himawan Putranta, Abdul Aziz Nur Rohman, Ernasari, Rida Siti Nur'aini Mahmudah, Wipsar Sunu Brams Dwandaru. "A simple distance measurement instrument based on the law of light reflection", Physics Education, 2019 Publication	1%
4	arro.anglia.ac.uk Internet Source	1%
5	W S B Dwandaru, A Fathia, R I Wisnuwjaya. "Study on the Synthesis of GO-AgNP Mixture Assisted by AgNP Based on UV-Vis, SEM-EDX, XRD, and FTIR", Journal of Physics: Conference Series, 2018	1%

	Publication	
6	Giuseppe Schirripa Spagnolo, Adriana Postiglione, Ilaria De Angelis. "Simple equipment for teaching internal photoelectric effect", Physics Education, 2020 Publication	1 %
7	china.iopscience.iop.org Internet Source	1 %
8	Koustav Konar, Kingshuk Bose, R. K. Paul. "Revisiting cosmic microwave background radiation using blackbody radiation inversion", Scientific Reports, 2021 Publication	1 %
9	lib.dr.iastate.edu Internet Source	1 %
10	www.scilit.net Internet Source	<1 %
11	iopscience.iop.org Internet Source	<1 %
12	N. F. Lubis, P. M. Widartiningsih, S. Viridi. "Numerical and Experimental Study of Thermal Response of an Electrified Nickel Wire", Journal of Physics: Conference Series, 2019 Publication	<1 %

13	Zheqin Dai, Zhiheng Xu, Tianbao Wang, Yingzheng Fan, Yucheng Liu, Ran Yu, Guangcan Zhu, Xiwu Lu, Baikun Li. "In-situ oil presence sensor using simple-structured upward open-channel microbial fuel cell (UOC-MFC)", Biosensors and Bioelectronics: X, 2019 Publication	<1 %
14	Advances in Computer Vision and Pattern Recognition, 2015. Publication	<1 %
15	J F Bakker. "Assessment of induced SAR in children exposed to electromagnetic plane waves between 10 MHz and 5.6 GHz", Physics in Medicine and Biology, 06/07/2010 Publication	<1 %
16	www.frontiersin.org Internet Source	<1 %
17	www.mdpi.com Internet Source	<1 %
18	Jonathan M. Marr, Francis P. Wilkin. "A better presentation of Planck's radiation law", American Journal of Physics, 2012 Publication	<1 %
19	S W Allison, D L Beshears, M R Cates, M B Scudiere, D W Shaw, A D Ellis. "Luminescence of YAG:Dy and YAG:Dy,Er crystals to 1700 °C", Measurement Science and Technology, 2020	<1 %

Publication

Exclude quotes	Off	Exclude matches	Off
Exclude bibliography	On		

C10_PE_Non-Contact_Temperature_Measurement.pdf

GRADEMARK REPORT

FINAL GRADE

/100

GENERAL COMMENTS

Instructor

PAGE 1

PAGE 2

PAGE 3

PAGE 4

PAGE 5

PAGE 6

PAGE 7

PAGE 8

PAGE 9

PAGE 10